Biocompatibility and corrosion resistance in biological media of hard ceramic coatings sputter deposited on metal implants

C. Sella and **J. C. Martin**
Laboratoire de Physique des Matériaux (CNRS), Meudon (France)

J. Lecoeur and **A. Le Chanu**
Laboratoire d'Electrochimie Interfaciale (CNRS), Meudon (France)

M. F. Harmand and **A. Naji**
INSERM, Université de Bordeaux II (INSERM U 36), Bordeaux (France)

J. P. Davidas
Société Française des Biomatériaux et Systèmes Implantables, Paris (France)

Abstract

The corrosion resistance and the biocompatibility of Ni–Cr, Co–Cr and titanium metal implants can be strongly enhanced by hard ceramic coatings (Al_2O_3, SiC etc.).

The corrosion resistance is evaluated through potentiodynamic polarization tests. The biocompatibility of coated and uncoated metals is compared using differentiated human cell cultures.

1. Introduction

Most metals used for orthopaedic and stomatology implants and prostheses belong to the families of titanium or nickel-based and cobalt-based superalloys designed for advanced technology industries (*e.g.* space, aeronautic and nuclear industries). Ideal materials should be as insoluble and biologically compatible as possible.

In the last 10 years, many accelerated *in vitro* corrosion tests have shown that nickel-based alloys are susceptible to corrosion when in contact with biological fluids (saliva and plasma). Recent studies [1] indicate the presence in dental tissues and gingivae of metal transferred from Ni–Cr dental metal implants. Released metal may be transported through body fluids to remote tissues (liver, spleen, brain, hair and nails), inducing cytotoxic and allergic effects. Patients receiving permanent metal implants (such as total hip joint replacements, osteosynthesis plates and nails or dental implants) show, within a short term, an important increase in metal content in the serum, blood and urine (up to two orders of magnitude higher than the normal levels). These high levels remain steady during the entire implantation time and decrease very slowly after removing the prosthesis [1].

2. Corrosion behaviour of metal implants in biological media

2.1. Experimental technique

The corrosion resistance was evaluated from potentiodynamic current–potential (I–E) curves. A standard three-electrode system was used (Fig. 1). The working electrode was the specimen, the reference electrode with a constant potential was a saturated calomel electrode (SCE) and the counterelectrode was made of vitreous carbon. The potential was imposed on the working electrode *vs.* the reference electrode and the current flowing between the specimen and the counterelectrode was recorded continuously on a linear scale. The potential range used was between -1.2 and $+1.6$ V (SCE), and the scan rate was 20 mV s^{-1}.

Two types of specimen holder have been used. The first (Fig. 2(a)) was used in the case of an uncoated sample. The dipping technique was applied, so that only the surface was in contact
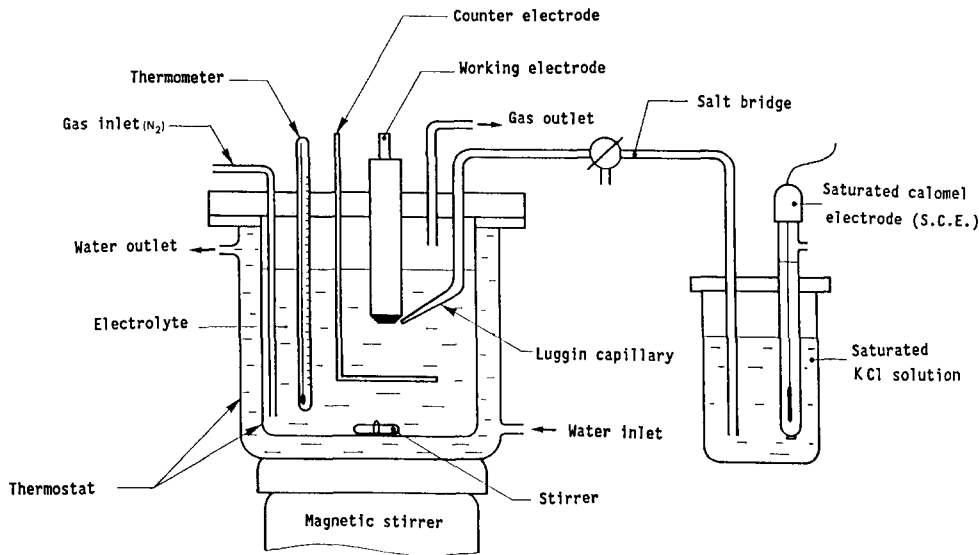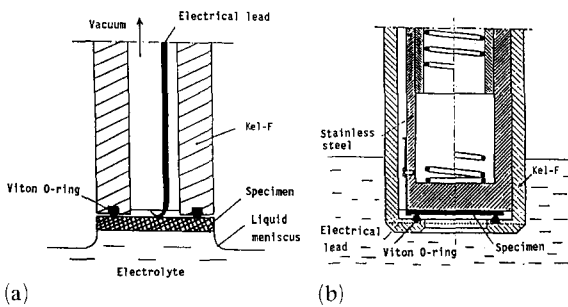
Fig. 1. Electrochemical cell.

(a)   (b)

Fig. 2. Specimen holder.

TABLE 1

Compositions of artificial saliva and synthetic blood plasma used in the *in vitro* experimentation

Artificial saliva		Synthetic blood plasma	
Constituent	Amount per 1000 g of ultrapurified water (g)	Constituent	Amount per 1000 g of ultrapurified water (g)
Na_2HPO_4	0.260	NaCl	6.800
NaCl	0.700	$CaCl_2$	0.200
KSCN	0.330	KCl	0.400
KCl	1.200	$MgSO_4$	0.100
KH_2PO_4	0.200	$NaHCO_3$	2.200
$NaHCO_3$	1.500	Na_2HPO_4	0.126
		NaH_2PO_4	0.026

with the solution. The second (Fig. 2(b)) was used with coated specimens; the O-ring means that only the surface was in contact with the electrolyte.

This technique [2] permits one to study many experimental conditions: for metals, the chemical composition, casting, heat treatment, internal stresses, machining, grinding, sandblasting, surface quality, roughness, superficial contamination, coating defects etc.; for solutions, the chemical composition, temperature, pH, aeration, stirring, organic or biological substance adsorption etc.

Test specimens consisted of disks with a thickness of 1–3 mm and a diameter of 12 mm. For some of them the surface was rough cast; for others the surface was polished to a mirror finish using standard metallographic techniques, with fine diamond pastes down to 1 μm. The specimens were studied using a scanning electron microscope, both before and after corrosion tests. A compositional analysis was made for each specimen using an electron probe microanalyser.

The *in vitro* experimentation required the use of artificial saliva and synthetic blood plasma maintained at 37 °C. The compositions of these solutions are shown in Table 1. These solutions were either oxygenated by air bubbling or oxygen depleted by nitrogen bubbling.

Metal corrosion in biological electrolytes, such as saliva and plasma, is mainly due to electro-

chemical processes resulting from the occurrence of several oxidation reactions simultaneously. Anodic surface reactions are not always corrosion reactions; partial oxidation of some products of the solution can occur, and the measured current corresponds to the addition of both an oxidation and a corrosion current.

2.2. Results

In the case of nickel-based alloys, including a wide variety of compositions having a nickel content ranging between 64 and 74 wt.% and a chromium content of 16–22 wt.%, the shape of the potentiodynamic polarization curve strongly depended on the composition. The passivation range was short and an important hysteresis was observed (Fig. 3(a)).

Co–Cr–Mo stellites form a more homogeneous group; their compositions and microstructures were very close and all polarization curves were very similar. No hysteresis was observed (Fig. 3(b)).

After electrochemical corrosion, the surface of the Ni–Cr alloy was covered by a thick layer of corrosion products (Fig. 4). After removal of this layer, corrosion pits were observed (Fig. 5),
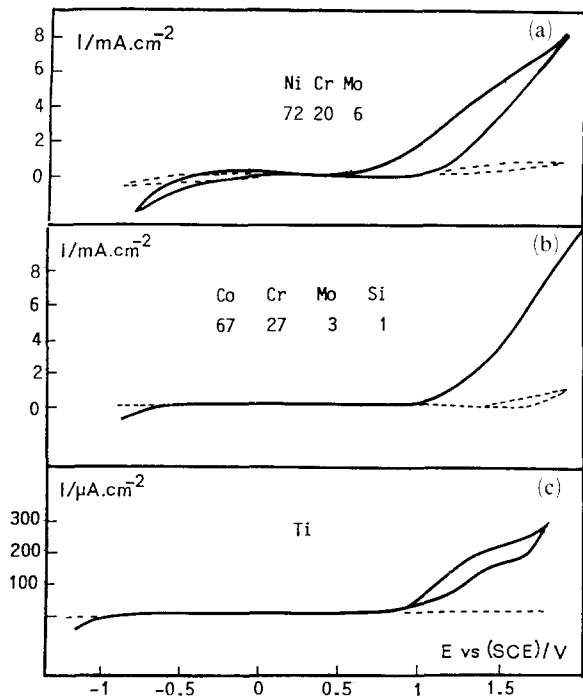
particularly in the case of alloys having a low chromium content and no molybdenum. The addition of molybdenum enhanced the resistance to pitting.

For Co–Cr–Mo alloys, the addition of molybdenum and an increase in the chromium content greatly enhanced the resistance to pitting and crevice corrosion; no pits were observed
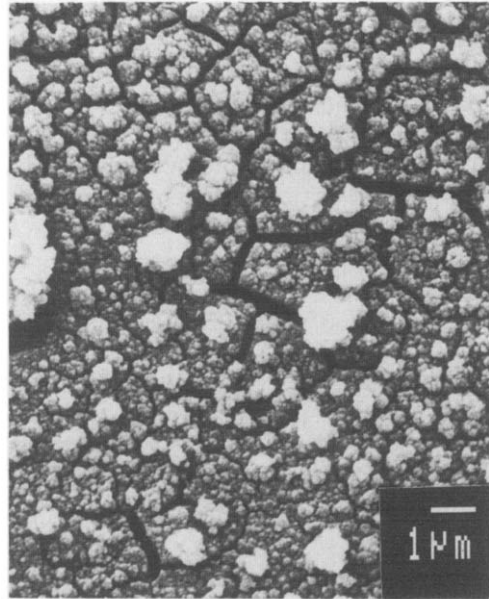

Fig. 4. Corrosion product layer on a 66wt.%Ni–22wt.%Cr–9wt.%Fe alloy (SP 20) after many polarization cycles in artificial saliva.

Fig. 3. Potentiodynamic *I–E* curves in artificial blood plasma (*T* = 37 °C; pH 6.7) for Ni–Cr, Co–Cr–Mo and titanium: ——, uncoated metal; ----, SiC- or Al₂O₃-coated metal.
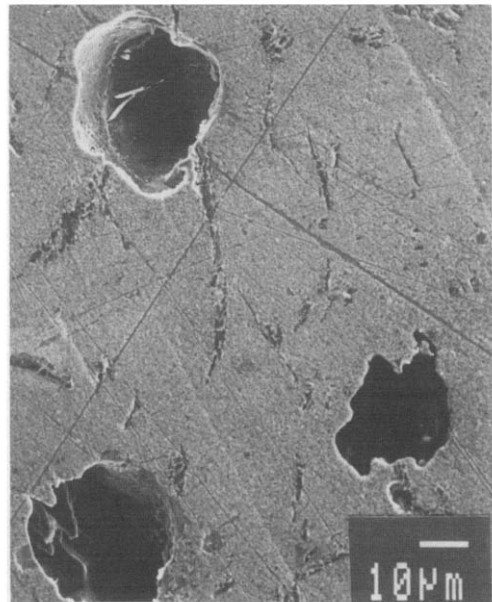

Fig. 5. Corrosion pits observed after removal of the corrosion product layer (SP 20).

after electrochemical corrosion. However, intergranular molybdenum- and chromium-rich precipitates were observed in relief since the corrosion rate was lower within these precipitates than on the metal grains (Fig. 6).

It can be noticed that, in comparison with the Ni–Cr and Co–Cr alloys, titanium exhibits a superior corrosion resistance as it has a larger passive range as well as very low current densities (Fig. 3(c)).

The potential range in the passive zone has to be compared with the potential within the oral cavity, which may vary considerably from -0.5 V (SCE) for anaerobic conditions to $+0.5$ V (SCE) for aerated environments, with an average value of 0.07 V (SCE) [3].

These accelerated *in vitro* corrosion tests show that nickel-based alloys are susceptible to corrosion when in contact with biological fluids (saliva and plasma), which suggests that they should not be used as permanent implant material.

For Co–Cr alloys, the corrosion resistance is significantly superior to the Ni–Cr and stainless steels previously used. However, in the presence of serum proteins, these alloys do release corrosion products in sufficient quantity to elicit biological responses [1].
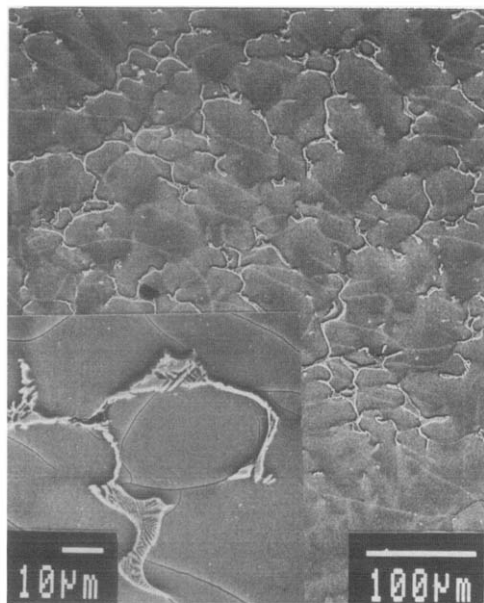

Fig. 6. Surface aspects of a Co–Cr–Mo alloy after removal of the corrosion product layer. The corrosion rate within molybdenum-rich precipitates (in relief) is lower than on the metal grains.

3. Protective coatings

3.1. Methodology

Ceramic implants (*e.g.* Al_2O_3 and vitreous carbon) have a well-known biocompatibility, but their brittleness and their difficult adaptation to the physiological requirements are major drawbacks. Therefore hard ceramic coatings deposited by r.f. sputtering on metal implants were tested as protective coatings to screen body fluids from the metal. Their protection efficiency was evaluated from the potentiodynamic current potential curves (Fig. 3 and Table 2).

The ceramic coatings tested were chosen from hard oxides, nitrides and carbides: Al_2O_3, SiO_2, AlN, TiN, SiC and WC. The best results were obtained with those having both a high Vickers hardness up to 3000 HV and good insulating properties (resistivity up to 10^{19} $\mu\Omega$ cm). That is the case for Al_2O_3 and SiC; BN and Si_3N_4 are also good candidates and are in the process of being evaluated.

The r.f. sputtering unit was equipped with two separate planar targets: one was used for depositing the ceramic coating, and the other for intermediate layers. A rotating substrate holder was used, with a target substrate distance of 5–10 cm. The base pressure was 10^{-4} Pa, and the sputtering pressure 0.7 Pa.

Al_2O_3 coatings were sputtered from a hot-pressed Al_2O_3 target (purity, 99%). SiC coatings were prepared by two methods: (1) sputtering in pure argon of a pressed target of SiC (purity, 99.5%); (2) reactive sputtering of a silicon target using a mixture of argon and 10% CH_4 as the

TABLE 2

Comparison of the protection efficiency of different coatings

Sample	Corrosion current at $E = 1.4$ V (ECS) $(\mu A \, cm^{-2})$
Uncoated metal or alloy	
1 Ni–Cr	6000–8000
2 Co–Cr–Mo	8000
3 Ti	260
Experimental coatings	
4 SiC (1 μm) on Ti	0.6
5 SiC (1 μm) on Co–Cr	10000
6 Ti (1 μm) on Co–Cr	500
7 SiC (1 μm) + Ti (1 μm) on Co–Cr	28
8 Al_2O_3 (0.5 μm) on Co–Cr	1800
9 Al_2O_3 (0.5 μm) + Al–Al_2O_3 cermet on Co–Cr	40

sputtering gas. The deposition rates were of the order of 0.3–0.8 μm h^{-1}.

Titanium intermediate layers were sputtered from a pure titanium target. Al–Al$_2$O$_3$ cermet sublayers were deposited using a composite target consisting of an Al$_2$O$_3$ plate to which aluminium strips were fixed; their number varies according to the required composition.

A high load adherence test unit (Sebastian IV produced by the Quad Group) capable of testing high strength bonds between a coating and its substrate was used.

Testing is accomplished by first bonding a pre-epoxy-coated stud to the coating surface. A progressive load is then applied through the stud until failure of the bond. The final breaking strength is recorded.

3.2. Results and discussion

One of the main factors that govern the durability of coatings is the adhesion, particularly if the film or substrate is subject to corrosion. A strong correlation between adhesion and corrosion resistance of the coatings was observed.

The current densities measured at the same potential ($E = 1.4$ V (SCE)) allowed for a comparison of the protection efficiency of different coatings (Table 2).

For the uncoated Ni–Cr or Co–Cr alloys the current density was high (6000–8000 μA cm^{-2}), and 20–30 times lower for uncoated titanium (260 μA cm^{-2}).

SiC coatings deposited on titanium (sample 4) were extremely adherent (up to 90 MPa) and the current density at 1.4 V (SCE) dropped to a very low value (0.6 μA cm^{-2}), 400–500 times lower than with uncoated titanium (260 μA cm^{-2}).

If the SiC coating was not very adherent, e.g. when deposited on Co–Cr substrates (sample 5, giving a poor adhesion value of 10 MPa), crack propagation was observed and the SiC layer flaked off. The current density at 1.4 V (SCE) was then very high ($10\,000$ μA cm^{-2}). The main reason for this poor adherence is related to the formation of high residual stresses (compressive) due to the low value of the thermal expansion coefficient for the ceramic coating (7×10^{-6} K^{-1} for SiC or Al$_2$O$_3$) in comparison with that of the metal substrate (14×10^{-6} K^{-1} for Co–Cr).

This thermal mismatch effect is reduced significantly when using a titanium substrate (sample 4) or a titanium underlayer on Co–Cr (sample 7). In this case, the thermal expansion coefficient for

titanium is 8.5×10^{-6} K, the SiC coating was then very adherent (adhesion of 70 MPa) and the current density fell to 28 μA cm^{-2}.

For Al$_2$O$_3$ deposited on Co–Cr the adhesion value (30 MPa) was stronger than for SiC. The current density at 1.4 V (SCE) was considerably, although not completely, reduced (1800 μA cm^{-2}). Using an Al–Al$_2$O$_3$ cermet intermediate layer between the Co–Cr substrate and the Al$_2$O$_3$ coating, the interface stresses were reduced. For an Al–Al$_2$O$_3$ cermet having a metal volume fraction of 0.4–0.5 the value of the thermal expansion coefficient became comparable with that of Co–Cr; then the Al$_2$O$_3$ coating was strongly adherent (60 MPa) and the current density dropped drastically to 40 μA cm^{-2} (sample 9).

Figure 7 shows the cross-section of a metal implant protected by an Al$_2$O$_3$ coating. No signs of corrosion were observed after many polarization cycles in artificial plasma or saliva.

The behaviour of SiC deposited on foils submitted to deformation was tested using a special specimen holder [4], which enabled a known curvature of the sample to be applied. The Y shift on the axial micrometer screw results in a curvature of the sample. R, the radius of curvature, is related to the Y value by the relation given in Fig. 8.

The tests were carried out at $E_D = 1.6$ V (SCE) and $E_D = 1$ V (SCE). The current–time (I–t) curve (Fig. 9) showed that after each deformation the current increased, owing to the formation of
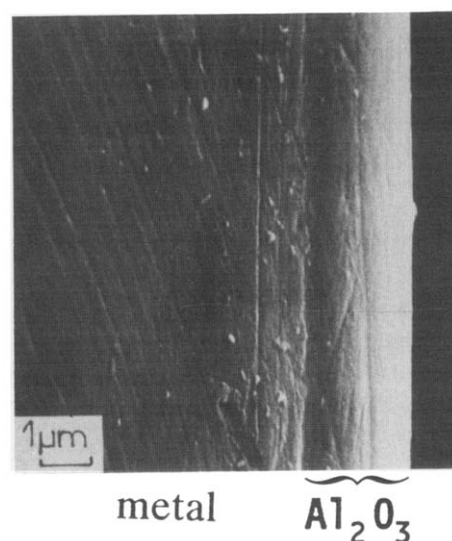

Fig. 7. Cross-section of an Al$_2$O$_3$-coated specimen (after corrosion tests; no interface defects and no intrinsic coatings defects).
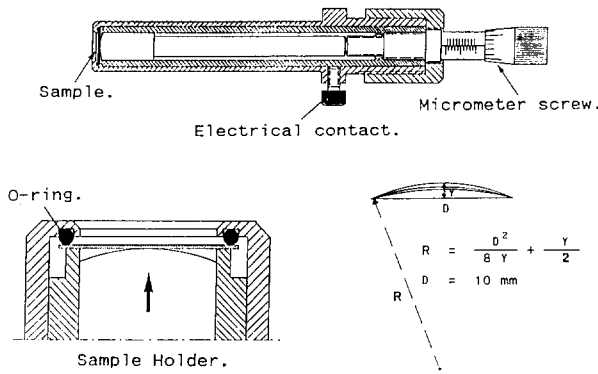
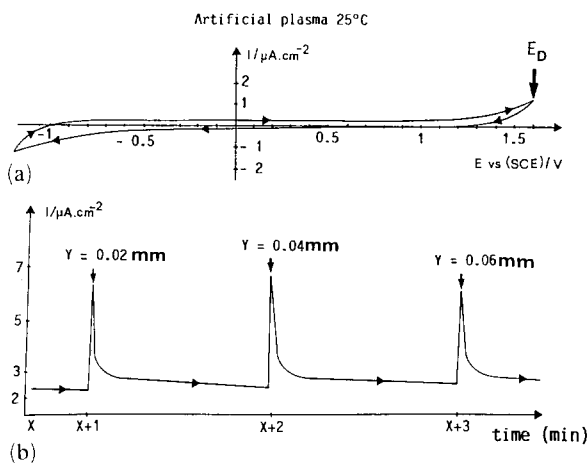Fig. 8. Specimen holder for the deformation tests in the electrochemical cell.

Fig. 9. Deformation test of an SiC-coated titanium foil (artificial plasma; 25 °C). (a) I-E curve for the coating before deformation. For the deformation test the potential is fixed at 1.6 V (SCE). (b) I-t curve. After each increase in displacement Y there is a current peak due to the formation of cracks, but after a very short time the passivation of titanium strongly reduces this current.
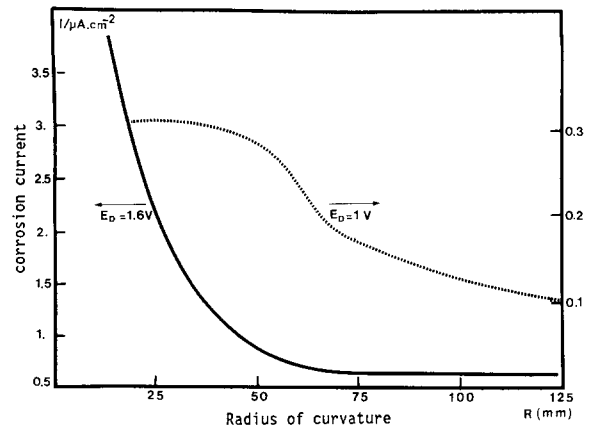

Fig. 10. Corrosion current vs. radius of curvature of an SiC coating deposited on a titanium foil 0.19 mm thick. The tests were carried out at $E_D = 1.6$ V and $E_D = 1$ V (SCE).

cracks, but after a very short time the passivation of the titanium substrate strongly reduced this current.

If the radius of curvature was higher than 50 mm, no change in the mean current value was observed (Fig. 10), but for a radius of curvature lower than 50 mm the intensity increased, owing to crack propagation in the protective layer. However, this current density remained very low ($0.2-3$ μA cm^{-2}) compared with that for an uncoated sample. So this is indirect evidence that the adhesion of the SiC coating on titanium is extremely high.

The wear resistance was found not only to be due to the hardness of the coating but also to depend on the adhesion. The wear test was performed by rubbing the surface with a cylindrical glass fibre pin (3 mm in diameter) under a load of 2 N corresponding to a contact pressure of 0.3 MPa.

For the best SiC coatings deposited on Co–Cr with a titanium underlayer (sample 7) it has been found that the wear rate is very small: 1 μm after 100 000 passages of the rubbing pin.

The structure of the films was deduced from transmission electron diffraction and electron microscopy studies performed on thinner SiC and Al$_2$O$_3$ films (500–1000 Å thickness) deposited onto carbon-coated copper grids. These studies showed that SiC and Al$_2$O$_3$ films had an amorphous structure and were perfectly continuous without any porosity.

That is why these sputtered coatings perform better than those deposited by plasma-spraying techniques in which coatings are usually associated with poor adherence and excessive porosity.

4. Cytotoxicity and biocompatibility testing

4.1. Methodology

During the past 20 years, biocompatibility tests have been carried out in vivo on animals (rats, rabbits, dogs, sheep and guinea pigs). However, the length of experimentation (about 2 years), the number of animals necessary to obtain a certain degree of reliability and a statistical approach to the results, and the high resulting cost, have led the experimenter to develop in vitro techniques for the evaluation of biocompatibility. Differentiated human cell cultures provide an excellent means of in vitro study of the interaction of the biological medium with the implantable material.
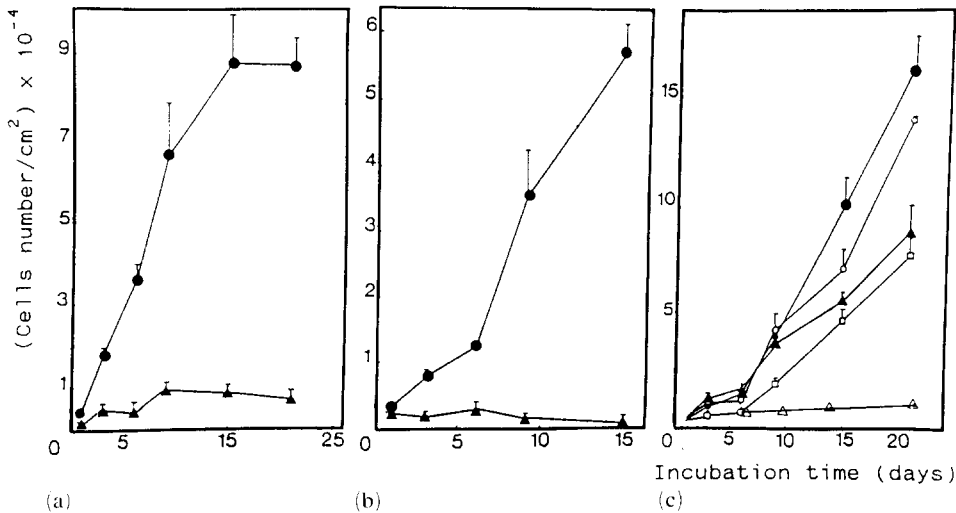
Fig. 11. (a) Cell proliferation curves of fibroblasts from gingival connective tissue on a Co-Cr disk (▲) and on the plastics of the culture well used as control (●). (b) Proliferation curves of osteoblast-like cells from alveolar bone on a Co-Cr disk (▲) and on the plastics used as control (●). (c) Proliferation curves of osteoblast-like cells from alveolar bone: titration of the toxic effect of extraction products obtained by electrochemical dissolution of Co-Cr alloys and added to the culture medium in two different dilutions (indirect tests): ▲, extraction solution Co-Cr (cobalt, 0.45 μg ml⁻¹; chromium, 0.25 μg ml⁻¹); △, extraction solution of Co-Cr (cobalt, 1.65 μg ml⁻¹; chromium, 0.75 μg ml⁻¹); ○, artificial saliva (as negative control); □, phenol, 64 μg ml⁻¹ (as positive control); ●, culture medium (as negative control).

Different aspects can be studied in agreement with the protocols described in various *AFNOR Standards* [5, 6]: viability (trypan blue exclusion test); mitotic function (cell proliferation and cell cycle phases); global metabolic activity (cell protein content); plasmic membrane integrity (evaluation of ^{51}Cr extracellular release); morphological study (cell morphology, cell mobility, cell attachment and spreading on the biomaterial); colonization of the material by the cell system; study of the cell differentiation (de-differentiation occurs when the material has poor biocompatibility, while a stimulation of the phenotype expression is observed when the material is biocompatible and bioactive); surface studies of the material in contact with the cell system (signs of corrosion etc.).

In the present paper, two human cell culture systems were used: osteoblast-like cells from alveolar bone, and fibroblasts from the gingival connective tissue [7].

Experiments were performed using multiwell culture plates (15.5 mm in diameter, NUNC) at 37 °C in a humidified atmosphere containing 5% CO_2. Two types of test were carried out.

(1) *Direct tests*. The cell suspension was cultivated on a disk of the material (15 mm in diameter and 1-2 mm thick) deposited at the bottom of each culture well. The initial cell density was about 5×10^3 cells cm^{-2}. The material used as control was the plastics of the culture well.
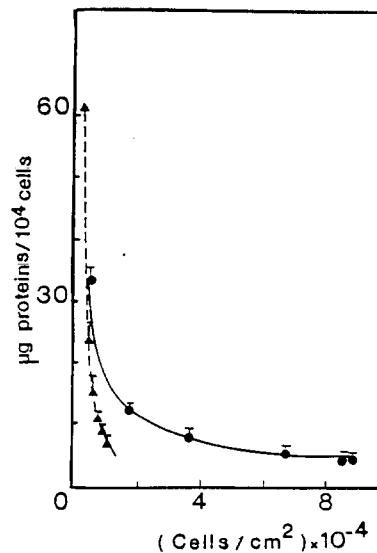

Fig. 12. Protein content of fibroblasts from gingival connective tissue cultivated on Co-Cr (▲) and on the plastics used as control (●).

(2) *Indirect tests*. Extraction solutions of metal were obtained by electrochemical dissolution according to *AFNOR Standard NFS 90-701* [5]. These extraction products were added to the culture medium in different dilutions, for the titration of the toxic effect. The metal content in the extracted solution was determined by atomic absorption spectroscopy.

4.2. Results

Different aspects of biocompatibility were studied [8]. Cell proliferation curves (Fig. 11) clearly showed that Co–Cr alloys were cytotoxic. Also, the cell protein content, which reflects the

Fig. 13. Culture of osteoblast-like cells from alveolar bone on a Co–Cr substrate (24 h).

metabolic state of the cells surviving on Co–Cr drops drastically from 60 μg per 10^4 cells to 5 μg per 10^4 cells. The protein content of the cells cultivated on the plastics used as control is twice that of the cells in contact with the metal (Fig. 12). The high toxicity of the alloy is illustrated in Fig. 13 showing a surviving cell after 24 h contact and in Fig. 14 indicating the presence of much cellular debris in the culture medium after contact for 3 days.

Al$_2$O$_3$ and SiC coatings were perfectly biocompatible and gave even better results than titanium (Fig. 15). Morphological studies confirmed perfect cell attachment and cell spreading on the ceramic coating (Fig. 16).

The *in vitro* corrosion and cytotoxicity tests were confirmed by clinical trials. Signs of corrosion have not been observed on any Al$_2$O$_3$-
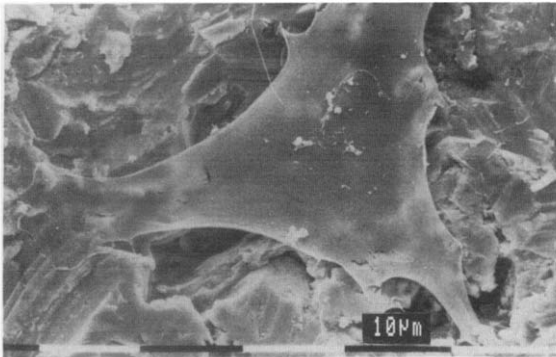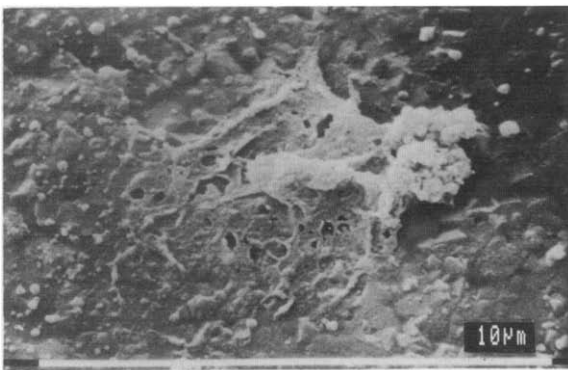

Fig. 14. Cellular debris after contact for 3 days on Co–Cr (osteoblast-like cells).
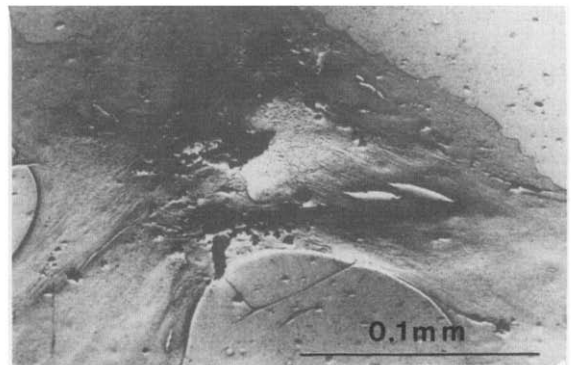

Fig. 16. Culture of osteoblast-like cells on an Al$_2$O$_3$ coating (3 days).
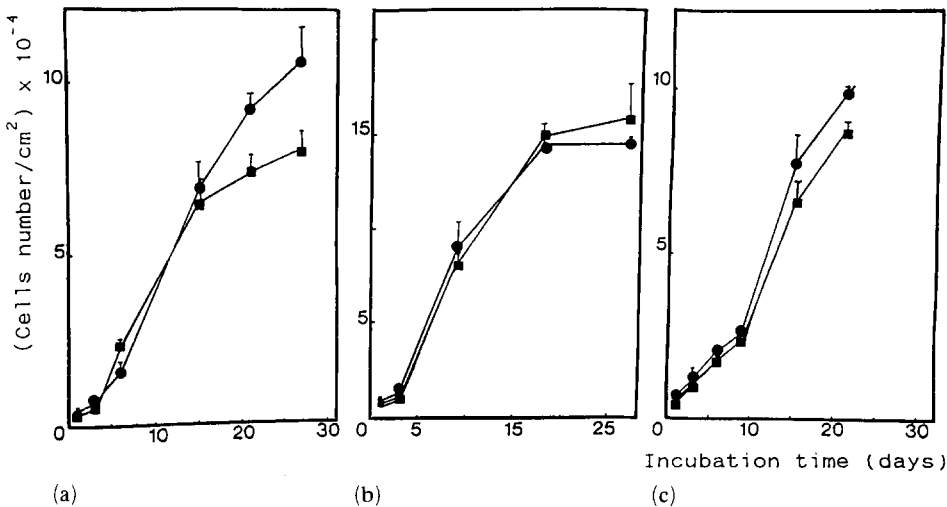

(a)   (b)   (c)

Fig. 15. Proliferation of osteoblast-like cells from alveolar bone (on the plastic used as control (●)): (a) on titanium (■); (b) on an Al$_2$O$_3$ coating (■); (c) on an SiC coating (■).

coated dental implants removed several years after implantation.

5. Conclusion

The biocompatibility and the corrosion resistance of metal implants can be strongly enhanced by hard ceramic coatings, which isolate body fluids from the metal perfectly.

Titanium intermediate layers improve the adherence for clinical use and act as an additional protection in case the ceramic coating is broken.

Acknowledgments

References

1 H. Hildebrand and M. Champy (eds.), *Biocompatibility of Co–Cr–Ni Alloys*, Plenum, New York, 1989.
2 Dental implants, Biocompatibility of dental metal alloys. Standardization of electrochemical tests, *AFNOR Stand. NFS 91-141*, 1988 (Association Française de Normalisation, Paris).
3 J. Ewers and M. R. Thorber, Corrosion of dental alloys in the oral environment, *Electroanal. Chem., 118* (1981) 275–290.
4 C. Sella, J. C. Martin, J. Lecoeur, J. P. Bellier, M. F. Harmand, A. Naji, J. P. Davidas and A. Le Chanu, Corrosion protection of metal implants by hard biocompatible ceramic coatings deposited by RF sputtering. *Clin. Mater., 5* (1990) 296–307.
5 Material and medical device biocompatibility. Extraction methods, *AFNOR Stand. NFS 90-701, 1988* (Association Française de Normalisation, Paris).
6 Study of cellular proliferation, *AFNOR Stand. NFS 91-142*, 1988 (Association Française de Normalisation, Paris).
  Study of total cellular proteins, *AFNOR Stand. 91-143*, 1988 (Association Française de Normalisation, Paris).
  Evaluation of 51 Cr extra-cellular release, *AFNOR Stand. 91-144*, 1988 (Association Française de Normalisation, Paris).
  Study of cell attachment and spreading on the biomaterial, *AFNOR Stand. 91-145*, 1988 (Association Française de Normalisation, Paris).
  Study of cellular multiplication, migration and adhesion, *AFNOR Stand. 91-146*, 1988 (Association Française de Normalisation, Paris).
7 M. F. Harmand, L. Bordenave, R. Duphil, R. Jeandot and D. Ducassou. Human differentiated cell cultures: *in vitro* models for characterization of cell/biomaterial interface, in P. Christel, A. Meunier and A. J. C. Lee (eds.), *Biological and Biomechanical Performance of Biomaterials*, Elsevier, Amsterdam, 1986, pp. 361–366.
8 A. Naji, Etude de la cytocompatibilité des biomatériaux. Comparaison entre lignées cellulaires et cellules différenciées d'origine humaine, *Thesis*, Université de Bordeaux, 1988.